THE AGES OF SINUS IRIDUM BASED ON CRATER DENSITIES.

Paula Dias[1] and Pedro Pina[1], [1]CERENA, Instituto Superior Técnico, Universidade de Lisboa, Av. Rovisco Pais, 1049-001 Lisboa, PORTUGAL (paula.dias@tecnico.ulisboa.pt, ppina@tecnico.ulisboa.pt).

Introduction: Lunar maria were emplaced over large periods of time, constituting different age units within the same large smooth plain [1]. The delineation of these units within volcanic plains has been performed using spectral data from different lunar missions, attempting to obtain accurate boundaries and estimations of the absolute model ages through crater size-frequency distribution (CSFD) measurements. For Sinus Iridum, a lunar mare filled crater of ~250 km in diameter located NW of Mare Imbrium, a substantial number of proposals of age units can be found in the literature [2-6]. Yet, due to the use of different data and processing procedures and interpretations, the mappings obtained show marked differences between them, not only in the amount of units detected but also on the location of the respective boundaries (Fig.1).

In order to overcome such large discrepancies, we have developed a more quantitative-based approach using impact crater densities [7]. It is inspired by previous works that used areal crater densities [8-9] and a randomness analysis of their spatial distribution to verify about the primary nature of the craters and the selection of the diameter intervals to use in the absolute age estimation procedure [10].

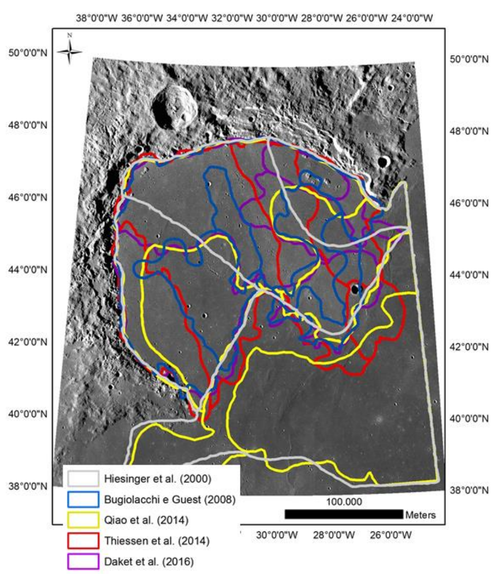

Fig.1. Age units of Sinus Iridum proposed by different authors [2-6], over a mosaic built from TC images of Kaguya [Image credits: USGS, Kaguya].

Data: We use a mosaic built from images of the Terrain Camera of Kaguya, with a spatial resolution of 7.4 m/pixel [11-12]. On this mosaic, all craters with a diameter D>500m were identified, being the obvious clusters and alignments of craters (secondary) not considered in the following steps. The resulting set is constituted by 1316 primary craters with the size distribution shown in Fig.2.

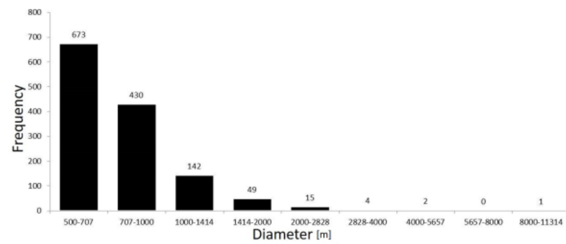

Fig.2. Size distribution of primary craters D>500m identified in Sinus Iridum.

Method: The processing chain is based on 3 main steps [7]: 1. Computation of areal crater densities (ACD) using a moving neighbourhood technique; 2. Determination of the boundaries between regions with distinct densities, using the watershed transform as segmentation tool; 3. Verification of the spatial randomness for each crater diameter bin within each delineated region, based on the measure M2CND-*Mean 2nd-closest neighbour distance* [10].

Mapping and dating: The parameters selected in each step of the procedure are the following:

1. ACD computation: search radius r=1200 m and output square cell c=500 m (Fig.3a).
2. Watershed transform, levels [0-100]: scale S=40 and merge M=5 (Fig.3b).
3. Spatial randomness verification: histograms built from 3000 iterations of Monte Carlo simulation of an equivalent set of craters and acceptance of diameter bins whose M2CND measure lies within the standard-deviation interval [-3σ, 3σ] of the mean, using Craterstats 2.0 [13] (Fig.3c).

The absolute ages were derived for each of the 6 identified regions (Fig.3b) using the lunar production function (PF) and the chronology function (CF) presented by Neukum et al. [14]. An example of this estimation for one the segmented units is shown in Fig.4.

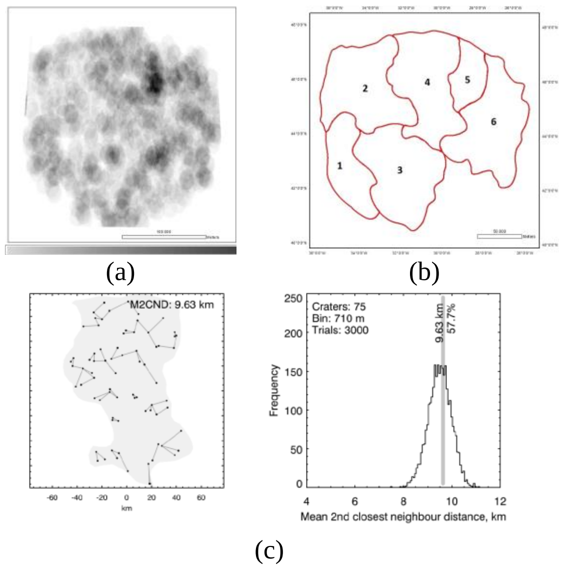

Fig.3. Main steps of the proposed method: (a) ACD map; (b) Segmentation of regions with similar ACD; (c) Verification of the spatial randomness for one crater diameter bin (710m) within one unit (region 4).

In addition, we used the raster LOLA Digital Elevation Model LDEM-256 to validate the segmentation by tracing several profiles along the regions detected. In the analysis of each stratigraphic profile, we were able to verify that the overlying layers of basalts are successively more recent. This way, Sinus Iridum can be constituted by 4 distinct geological units of ages 3.74 Ga (unit 4), 3.45~3.42 Ga (units 5 and 1), 3.26 Ga (unit 2) and 3.17 Ga (units 3 and 6) (Fig.5).

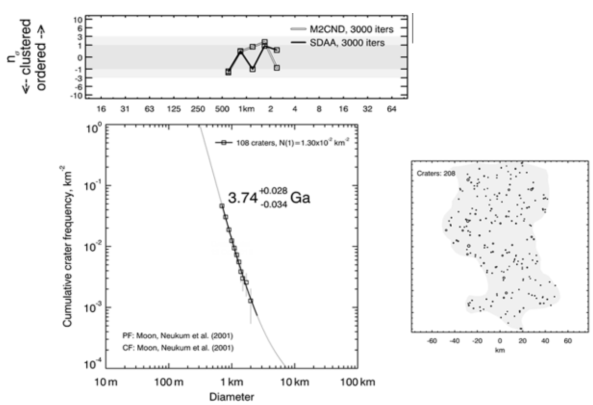

Fig.4. Dating procedure (region 4): Summary plot for randomness verification in each diameter bin, CSFD measurements and map of craters used.

Conclusions: The integration of a robust segmentation tool with other quantitative approaches permits disposing of a processing sequence where subjective evaluations are substantially reduced in the determination of the boundaries of units in volcanic smooth plains of the Moon. We have also applied this same procedure using smaller primary craters (D>50m), but only in transition zones (900 km^2 squared regions) of the boundaries detected before, to verify the possibility of enhancing even more the level of detail. But the results are so far inconcluse: in half of these test zones, sub-units with homogeneous crater densities were clearly detected, also replicating the same previous boundary (D>500m), but in the other half this was not so evident. This uncertainty may result from working with too small transitions zones and also from not detecting all secondary craters. The validation of all automated detections D>50m in the whole Sinus Iridum plain [15] to make available a larger crater dataset, together with the development of a reliable and objective tool to detect secondaries, will certainly allow a more sustained conclusion.

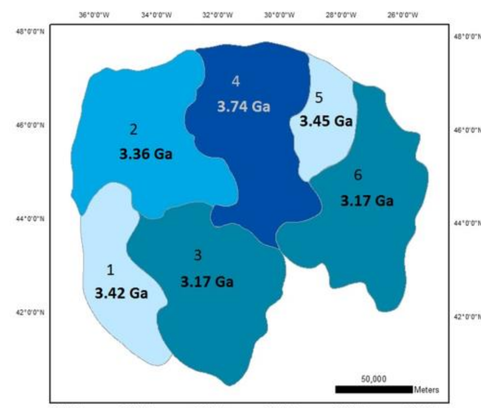

Fig.5. Age units of Sinus Iridum obtained with the crater densities based approach.

References: [1] Hartmann W. K. et al. (1981) In *Basaltic Volcanism in Terrestrial Planets*, 1049-1127. [2] Hiesinger H. et al. (2000) *JGR* 105: 29329-29275. [3] Buggiolacchi R. and Guest J. E. (2008) *Icarus* 197: 1-18. [4] Qiao L. et al. (2014) *PSS* 101: 37-52. [5] Thiessen F. et al. (2014) *PSS* 104: 244-252. [6] Daket Y. et al. (2016) *EPS* 68: 157. [7] Dias P. and Pina P. (2017), Segmentation of lunar maria based on crater densities, watershed transform and spatial randomness analysis, *Lunar and Planetary Science Conference XLVIII*, abstract #1836. [8] Ostrach L. R and Robinson M. S. (2013) *LPSC XLIV*, abstract #1086. [9] Ostrach L. R. and Robinson M. S. (2014) *LPSC XLV*, abstract #1266. [10] Michael G. G. et al. (2012) *Icarus* 218: 169-177. [11] Kato M. et al. (2006) *LPSC XXXVII*, abstract #1233. [12] Isbell C. et al. (2014) *LPSC XLV*, abstract #2268. [13] Craterstats 2.0 software, FU Berlin. [14] Neukum G. et al. (2001), *Space Sci. Rev.*, 96, 55–86. [15] Machado M. et al. (2015) *LPSC XLVI*, abstract #1797.